Electronic Supplementary Information

Amplified circularly polarized luminescence of chiral lanthanide-based chains through helical assembly

Xue-Ting Wang,[1] Fang-Wen Lv,[1] Hang Qin,[2] Xin-Tong Dai,[2] Shan Jin,[*1] and Xiu-Ying Zheng[*1]

[1] Institutes of Physical Science and Information Technology, Key Laboratory of Structure and Functional Regulation of Hybrid Materials of Ministry of Education, Anhui University, Hefei, 230601, P. R. China.

[2] School of Materials Science and Engineering, Anhui University, 230601, P. R. China

Email: jinshan@ahu.edu.cn, xyzheng@ahu.edu.cn

Materials and Physical Measurements.

All reagents were commercially available and were used without further purification. **Caution!** An aqueous solution of $Ln(ClO_4)_3$ (1.0 M) was prepared by the reaction of Ln_2O_3 (Ln = Eu, Tb) and perchloric acid (70.0% – 72.0%) in the fume cupboard. Elemental analyses (EA) (C, H and N) were carried out using a Vario EL–3 elemental analyzer. The infrared spectrum was recorded on a VERTEX 80 FT–IR Spectrophotometer with pressed KBr pellets. A Rigaku Ultima IV Powder X-ray diffractometer verified the purity and stability of the power sample. The fluorescence data were collected by Horiba Fluoro max plus. The decay lifetimes were recorded on Horiba Fluoro max plus with micro-second pulse lamp as the excitation source. The quantum yields were recorded on spectrofluorometer FS 5. Powder samples of the chiral compounds and KBr were mixed in a mortar and ground thoroughly using a pestle. The resulting mixture was compressed under a pressure of 10 MPa to form a thin dict. The intrinsic circularly polarized luminescence (CPL) spectra were measured on JASCO CPL-300 spectrometer with pressed KBr pellet. The circular dichroism (CD) spectra were measured using JASCO J-1700 circular dichroism spectrometer with pressed KBr pellet. Magnetic measurements (2 – 300 K) were investigated for powdered samples on a Quantum Design SQUID MPMS-XL magnetometer.

X-ray crystallography. The crystal data of compounds ***R*/*S*-Ln** and ***R*/*S*-Ln-phen** (Ln = Eu/Tb) were collected on a STOE STADIVARI detector with Cu K_α radiation (λ = 1.54184 Å) at 120 K. Absorption corrections were applied by using the multi-scan program STOE LANA. The structures were solved by direct methods, and non-hydrogen atoms were refined anisotropically by least-squares on F^2 using the OLEX2 program.[1-2] The hydrogen atoms of organic ligands were generated geometrically (C–H, 0.96 Å). Crystal data as well as details of data collection and refinement for the complexes are summarized in Tables S1-S2. Selected bonds are showed in Tables S3-S10. These disorder solvent molecules were removed using SQUEEZE.[3] CCDC numbers of 2379931-2379938 for ***R*/*S*-Ln** and ***R*/*S*-Ln-phen** (Ln = Eu/Tb) can be obtained free of charge from http://www.ccdc.cam.ac.uk/data_request/cif.

Synthesis of {[Eu(*R*-L)$_2$(H$_2$O)$_2$]·(ClO$_4$)}$_n$ (*R*-Eu).

(*R*)-alpha-Methoxyphenylacetic acid (*R*-HL, 0.5 mmol, 83 mg), Eu(ClO$_4$)$_3$(1.0 mL, 1.0 M)were dissolved in MeCN (10.5 mL). Then, Freshly prepared NaOH (1200 μL, 1.0 M) was added dropwise with stirring. The resulted mixture quickly became turbid, and then gradually clarified in a short time under vigorous stirring. After heating and stirring at approximately 130℃ for 3 h, the mixture was filtered and evaporated under ambient conditions. After approximately 2 weeks, the colorless block crystals were obtained (yield 11% based on Eu(ClO$_4$)$_3$). Anal. Calcd (%) for $C_{18}H_{22}ClEuO_{12}$ (FW = 617.76): C: 34.99, H: 3.59. Found (%): C: 34.23, H: 3.57. Selected IR peaks (cm^{-1}): 3420 (s), 2975 (w), 2948 (w), 1653 (s), 1594 (w), 1441 (s), 1347 (m), 1305 (w), 1264 (w), 1194 (w), 1136 (w), 1085 (w), 1055 (w), 984 (w), 962 (w), 922 (w), 793 (w), 738 (w), 703 (w), 624 (w), 594 (w), 526 (w).

Synthesis of {[Eu(*S*-L)$_2$(H$_2$O)$_2$]·(ClO$_4$)}$_n$ (*S*-Eu).

Compound ***S*-Eu** was prepared using the same procedures as described above for the synthesis of ***R*-Eu** but using (*S*)-alpha-Methoxyphenylacetic acid (*S*-HL) to replace *R*-HL. After approximately 2 weeks, the colorless block crystals were obtained (yield 11% based on Eu(ClO$_4$)$_3$). Anal. Calcd (%) for $C_{18}H_{22}ClEuO_{12}$ (FW = 617.76): C: 34.99, H: 3.59. Found (%):C: 34.19, H: 3.58. Selected IR peaks (cm^{-1}): 3420 (s), 2975 (w), 2948 (w), 1653 (s), 1594 (w), 1441 (s), 1347 (m), 1305 (w), 1264 (w), 1194 (w), 1136 (w), 1085 (w), 1055 (w), 984 (w), 962 (w), 922 (w), 793 (w), 738 (w), 703 (w), 624 (w), 594 (w), 526 (w).

Synthesis of {[Tb(*R*-L)$_2$(H$_2$O)$_2$]·(ClO$_4$)}$_n$ (*R*-Tb).

Compound ***R*-Tb** was prepared using the same procedures as described above for the synthesis of ***R*-Eu** but freshly made NaOH (1200 μL, 1.0 M) was replaced with freshly made NaOH (2100 μL, 1.0 M) and using Tb(ClO$_4$)$_3$ to replace Eu(ClO$_4$)$_3$. After approximately 2 weeks, the colorless block crystals were obtained (yield 10% based on Tb(ClO$_4$)$_3$). Anal. Calcd (%) for $C_{18}H_{22}ClTbO_{12}$ (FW = 624.72): C: 34.60, H: 3.55. Found (%): C: 33.31, H: 3.51. Selected IR peaks (cm^{-1}): 3420 (s), 2975 (w), 2948 (w),

1653 (s), 1594 (w), 1441 (s), 1347 (m), 1305 (w), 1264 (w), 1194 (w), 1136 (w), 1085 (w), 1055 (w), 984 (w), 962 (w), 922 (w), 793 (w), 738 (w), 703 (w), 624 (w), 594 (w), 526 (w).

Synthesis of {[Tb(*S*-L)$_2$(H$_2$O)$_2$]·(ClO$_4$)}$_n$ (*S*-Tb).

Compound ***S*-Tb** was prepared using the same procedures as described above for the synthesis of ***R*-Tb** but using *S*-HL to replace *R*-HL. After approximately 2 weeks, the colorless block crystals were obtained (yield 10% based on Tb(ClO$_4$)$_3$). Anal. Calcd (%) for $C_{18}H_{22}ClTbO_{12}$ (FW = 624.72): C: 34.61, H: 3.55. Found (%): C: 33.28, H: 3.52. Selected IR peaks (cm^{-1}): 3420 (s), 2975 (w), 2948 (w), 1653 (s), 1594 (w), 1441 (s), 1347 (m), 1305 (w), 1264 (w), 1194 (w), 1136 (w), 1085 (w), 1055 (w), 984 (w), 962 (w), 922 (w), 793 (w), 738 (w), 703 (w), 624 (w), 594 (w), 526(w).

Synthesis of {[Eu$_2$(*R*-L)$_5$(phen)$_2$(H$_2$O)]·(ClO$_4$)·(H$_2$O)$_{0.5}$}$_n$ (*R*-Eu-phen).

R-HL (0.5 mmol, 83 mg), 1,10-Phenanthroline (phen, 0.2 mmol, 36 mg), Eu(ClO$_4$)$_3$(1.0 mL, 1.0 M) were dissolved in MeCN (10.7 mL). Then, Freshly prepared NaOH (500 μL, 1.0 M) was added dropwise with stirring. The resulted mixture quickly became turbid, and then gradually clarified in a short time under vigorous stirring. After heating and stirring at approximately 130 ℃ for 3 h, the mixture was filtered and evaporated under ambient conditions. After approximately 2 weeks, the colorless block crystals were obtained (yield 13% based on Eu(ClO$_4$)$_3$). Anal. Calcd (%) for $C_{69}H_{64}ClEu_2N_4O_{20.5}$ (FW = 1616.61): C: 51.26, H: 3.99, N: 3.47. Found (%): C: 51.08, H: 3.99, N: 3.19. Selected IR peaks (cm^{-1}): 3437 (s), 3070 (m), 2931 (m), 2830 (w), 1963 (w), 1585 (s), 1427 (w), 1334 (w), 1200 (w), 1092 (s), 980 (w), 856 (w), 725 (m), 613 (w).

Synthesis of {[Eu$_2$(*S*-L)$_5$(phen)$_2$(H$_2$O)]·(ClO$_4$)· (H$_2$O)$_{0.5}$}$_n$ (*S*-Eu-phen).

Compound ***S*-Eu-phen** was prepared using the same procedures as described above for the synthesis of ***R*-Eu-phen** but using *S*-HL to replace *R*-HL. After approximately 2 weeks, the colorless block crystals were obtained (yield 13% based on Eu(ClO$_4$)$_3$).

Anal. Calcd (%) for $C_{69}H_{64}ClEu_2N_4O_{20.5}$ (FW = 1616.61): C: 51.26, H: 3.99, N: 3.47. Found (%): C: 51.18, H: 3.97, N: 3.13. Selected IR peaks (cm^{-1}): 3437 (s), 3070 (m), 2931 (m), 2830 (w), 1963 (w), 1585 (s), 1427 (w), 1334 (w), 1200 (w), 1092 (s), 980 (w), 856 (w), 725 (m), 613 (w).

Synthesis of $\{[Tb_2(\boldsymbol{R}\text{-L})_5(phen)_2(H_2O)]\cdot(ClO_4)\cdot(H_2O)_{0.5}\}_n$ (*R*-Tb-phen).

Compound ***R*-Tb-phen** was prepared using the same procedures as described above for the synthesis of ***R*-Eu-phen** but freshly made NaOH (1210 μL, 1.0 M) was replaced with freshly made NaOH (500 μL, 1.0 M) and using $Tb(ClO_4)_3$ to replace $Eu(ClO_4)_3$. After approximately 2 weeks, the colorless block crystals were obtained (yield 12% based on $Tb(ClO_4)_3$). Anal. Calcd (%) for $C_{69}H_{64}ClTb_2N_4O_{20.5}$ (FW = 1630.53): C: 50.83, H: 3.96, N: 3.44. Found (%): C: 50.95, H: 3.93, N: 3.09. Selected IR peaks (cm^{-1}): 3437 (s), 3070 (m), 2931 (m), 2830 (w), 1963 (w), 1585 (s), 1427 (w), 1334 (w), 1200 (w), 1092 (s), 980 (w), 856 (w), 725 (m), 613 (w).

Synthesis of $\{[Tb_2(\boldsymbol{S}\text{-L})_5(phen)_2(H_2O)]\cdot(ClO_4)\cdot(H_2O)_{0.5}\}_n$ (*S*-Tb-phen).

Compound ***S*-Tb-phen** was prepared using the same procedures as described above for the synthesis of ***R*-Tb-phen** but using *S*-HL to replace *R*-HL. After approximately 2 weeks, the colorless block crystals were obtained (yield 12% based on $Tb(ClO_4)_3$). Anal. Calcd (%) for $C_{69}H_{64}ClTb_2N_4O_{20.5}$ (FW = 1630.53): C: 50.83, H: 3.96, N: 3.44. Found (%): C: 50.66, H: 3.96, N: 3.44. Selected IR peaks (cm^{-1}): 3437 (s), 3070 (m), 2931 (m), 2830 (w), 1963 (w), 1585 (s), 1427 (w), 1334 (w), 1200 (w), 1092 (s), 980 (w), 856 (w), 725 (m), 613 (w).

The detailed fitting procedure for the various optical parameters presented in Table 1.

τ_{obs}: the luminescence decay lifetime fitted by a mono-exponential function. $I(t) = I_0+A_1\exp(-t/\tau_{obs})$. $I(t)$, the fluorescence intensity versus time t. I_0, the initial luminescence intensity. A_1, the scalar quantity obtained upon curve fitting. t, the time.

τ_r: decay lifetime. $1/\tau_r = AM_{D,0}\, n^3(I_{tot}/I_{MD})$. $AM_{D,0}$, the Einstein coefficient of the MD transition equal to 14.65 s^{-1}. n, the refractive index. I_{tot}, a ratio of the total integrated emission. I_{MD}, the integrated intensityof the MD transition emission.

k_r: radiative decay rate constant. $k_r = 1/\tau_r$. τ_r, decay lifetime.

k_{nr}: non-radiative decay rate constant. $\tau_{obs} = 1/(k_r+k_{nr})$. k_r, radiative decay rate constant. τ_{obs}, the luminescence decay lifetime.

Φ_{Eu}: absolute emission photoluminescence quantum yield. $\Phi_{Eu} = \tau_{obs}/\tau_r$. τ_{obs}, the luminescence decay lifetime. τ_r, decay lifetime.

Φ_{tot}: the photoluminescence quantum yield.

η_{sens}: the sensitization efficiency. $\eta_{sens} = \Phi_{tot}/\Phi_{Eu}$. Φ_{tot}, the photoluminescence quantum yield. Φ_{Eu}, absolute emission photoluminescence quantum yield.

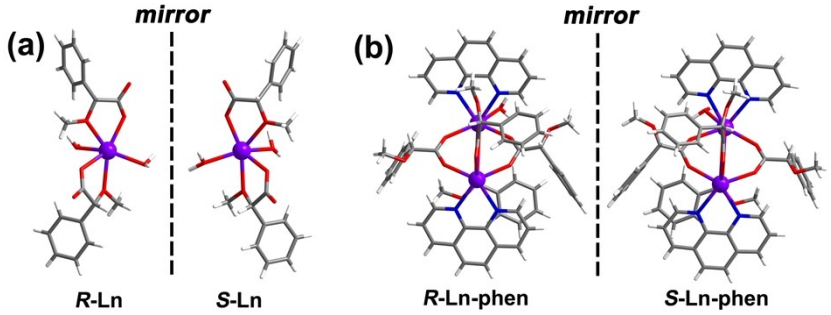

Fig. S1 (a) The asymmetric unit $[Ln(R/S\text{-}L)_2(H_2O)_2]^+$ in ***R*/*S*-Ln**; (b) the minimum repeat unit $[Ln(R/S\text{-}L)_4(phen)_2(H_2O)]^{2+}$ in ***R*/*S*-Ln-phen**.

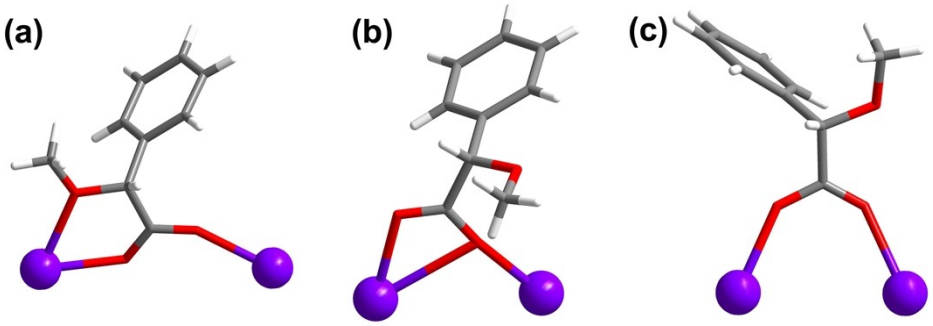

Fig. S2 The different bridging modes of $R/S\text{-}L^-$ with Ln^{3+} ions in ***R*/*S*-Ln** and ***R*/*S*-Ln-phen**.

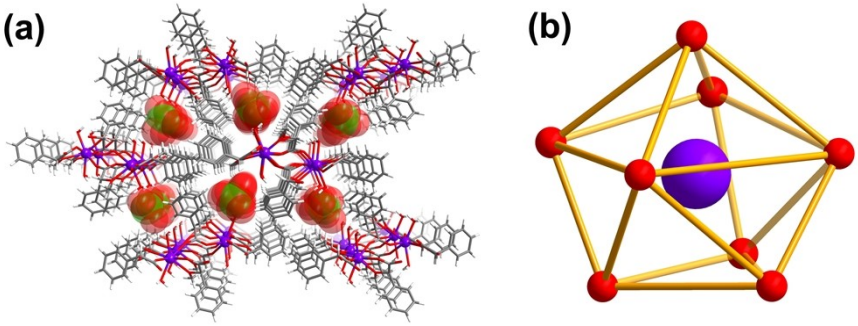

Fig. S3 (a) The 3D framework $\{[Ln(R/S\text{-}L)_2(H_2O)_2]\cdot(ClO_4)\}_n$ of 1D chain ***R*/*S*-Ln** formed by the hydrogen bond between the H atoms from the chain and the O atoms on free counter anion ClO_4^-; (b) the octa-coordinated Ln^{3+} in ***R*/*S*-Ln** featuring biaugmented trigonal prism geometric configuration.

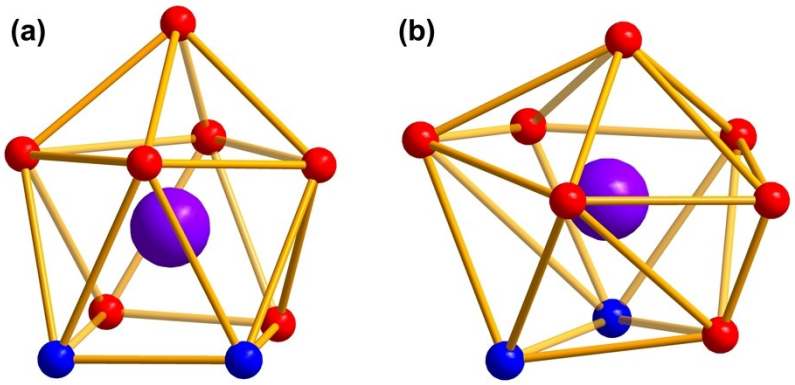

Fig. S4 For ***R*/*S*-Ln-phen**, the nine coordination mode of Ln^{3+} featuring (a) capped square antiprism geometry and (b) muffin geometry.

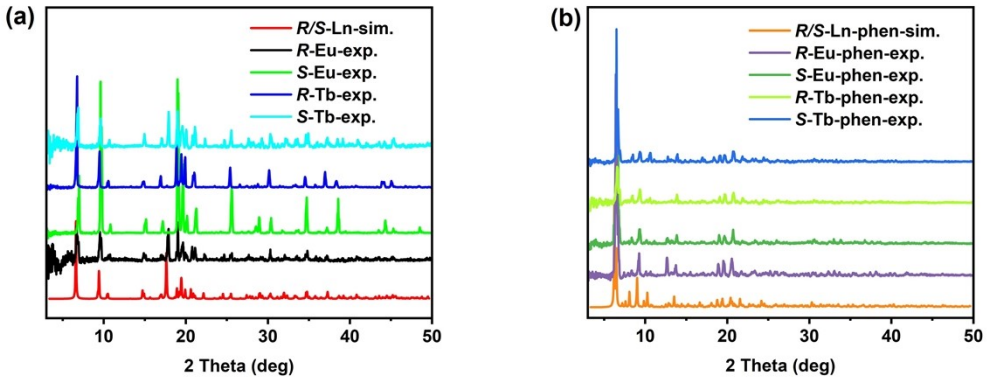

Fig. S5 (a) and (b) are the experimental and simulated PXRD spectra of ***R/S*-Ln** and ***R/S*-Ln-phen** (Ln = Eu/Tb), respectively.

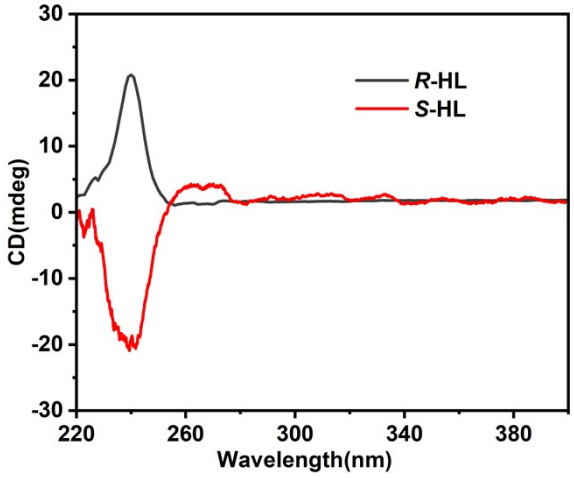

Fig. S6 The solid-state CD spectrum of chiral ligand *R*/*S*-HL.

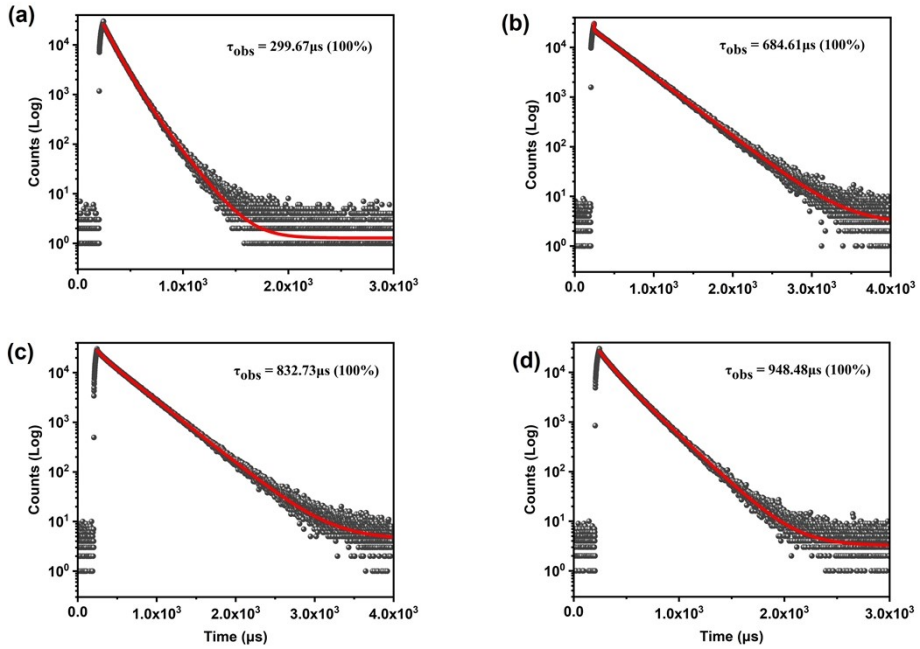

Fig. S7 The luminescence decay curves of (a) ***S*-Eu**, (b) ***S*-Tb**, (c) ***S*-Eu-phen** (d) ***S*-Tb-phen** fitted by a mono-exponential function.

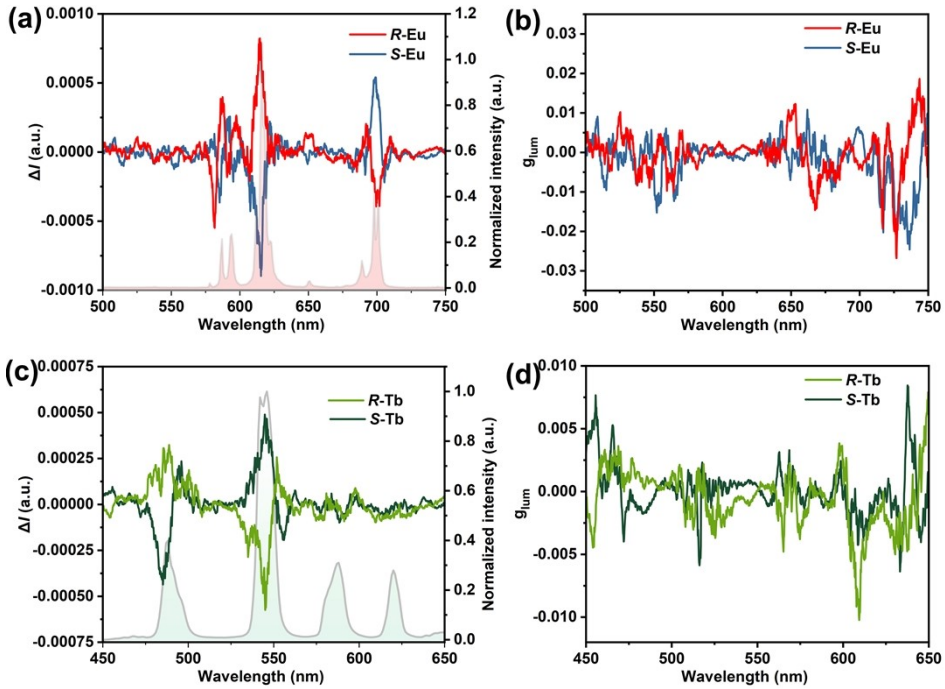

Fig. S8 (a) and (c) are the solid-state CPL spectra of ***R*/*S*-Eu** (λ_{ex} = 395 nm) and ***R*/*S*-Tb** (λ_{ex} = 370 nm), respectively. Normalized luminescence is traced in the background. (b) and (d) are the g_{lum} spectra of ***R*/*S*-Eu** and ***R*/*S*-Tb**.

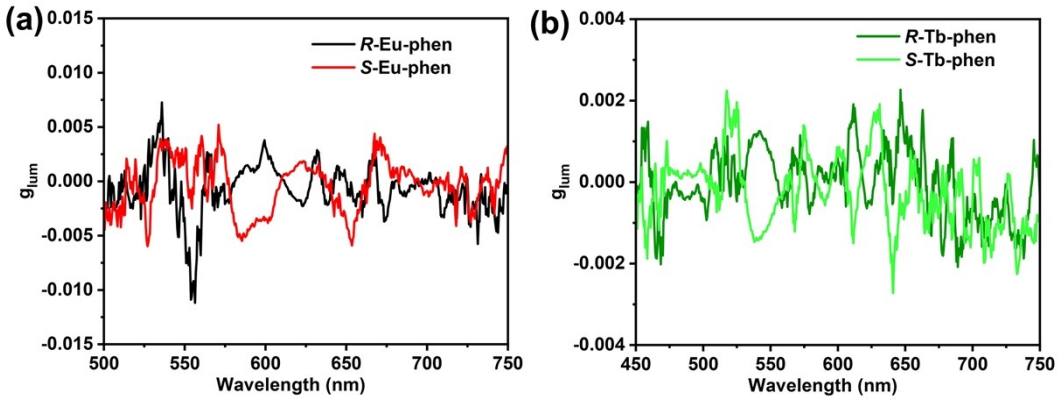

Fig. S9 The g_{lum} spectra of (a) ***R/S*-Eu-phen** and (b) ***R/S*-Tb-phen**.

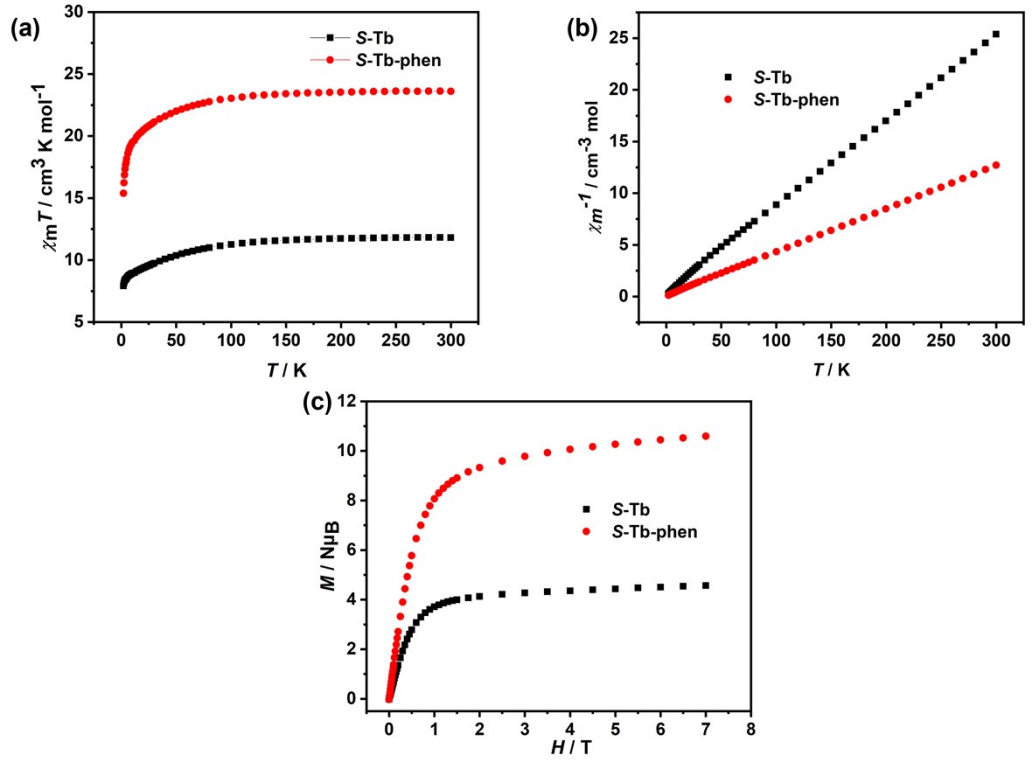

Fig. S10 (a) The magnetic susceptibility of ***S*-Tb** and ***S*-Tb-phen** was measured using the dried powder samples in the temperature range of 2 – 300 K and in a direct field of 1000 Oe; (b) the fitting of χ_m^{-1} vs T based on Curie-Weiss law for ***S*-Tb** and ***S*-Tb-phen**; (c) field dependence of the magnetization plots of ***S*-Tb** and ***S*-Tb-phen** at the indicated temperatures.

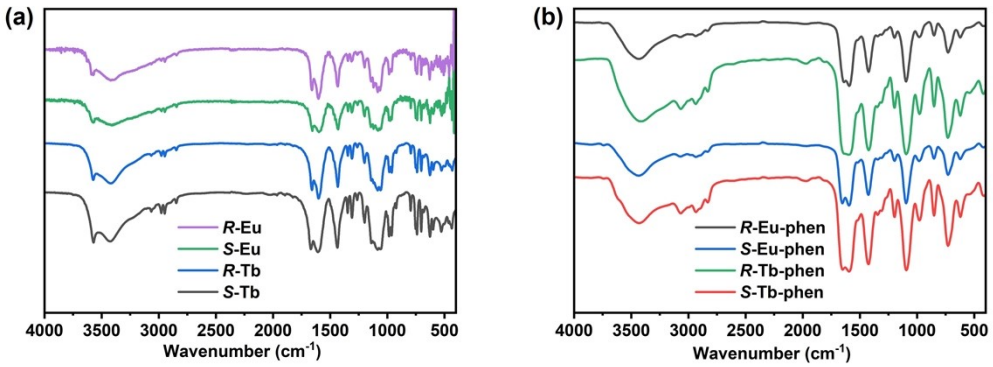

Fig. S11 (a) and (b) are the IR spectra of ***R/S*-Ln** and ***R/S*-Ln-phen** (Ln = Eu/Tb), respectively.

Table S1. Crystallographic data for compounds ***R*/*S*-Ln** (Ln = Eu/Tb).

Compound	***R*-Eu**	***S*-Eu**	***R*-Tb**	***S*-Tb**
Formula	$C_{18}H_{22}ClEuO_{12}$	$C_{18}H_{22}ClEuO_{12}$	$C_{18}H_{22}ClTbO_{12}$	$C_{18}H_{22}ClTbO_{12}$
FW	617.76	617.76	624.72	624.72
T/K	120	120	120	120
Cry. system	orthorhombic	orthorhombic	orthorhombic	orthorhombic
Space group	$P2_12_12_1$	$P2_12_12_1$	$P2_12_12_1$	$P2_12_12_1$
a /Å	6.2461(2)	18.7671(4)	18.7651(8)	18.7948(7)
b /Å	18.7509(5)	19.0219(3)	18.9706(10)	18.9335(7)
c /Å	19.0329 (4)	6.25350(10)	6.2102(3)	6.2122(3)
α/°	90	90	90	90
β/°	90	90	90	90
γ/°	90	90	90	90
V/Å^3	2229.13(10)	2232.41(7)	2210.74(18)	2210.62(16)
Z	4	4	4	4
ρ_c/g cm^{-3}	1.841	1.838	1.877	1.877
μ/ mm^{-1}	21.806	21.774	17.410	17.411
Data/parameters	4229/319	4108/296	3837/318	4000/319
2θ/°	6.618-155.568	6.616-138.834	9.324-132.942	6.626-138.744
Obs. reflections	4917	35515	10260	10911
F(000)	1224	1224	1232.0	1232..0
GOF	1.037	1.047	1.065	1.034
R_1[I> 2σ(I)][a]	0.0693	0.0252	0.0467	0.0429
wR_2(All data)[b]	0.1933	0.0592	0.1242	0.1149

[a] $R_1=\Sigma||F_O| - |F_C||/\Sigma|F_O|$; [b] $wR_2=\{\Sigma[w(F_O^2 - F_C^2)^2]/\Sigma[w(F_O^2)^2]\}^{1/2}$

Table S2. Crystallographic data for compounds ***R*/*S*-Ln-phen** (Ln = Eu/Tb).

Compound	***R*-Eu-phen**	***S*-Eu-phen**	***R*-Tb-phen**	***S*-Tb-phen**
Formula	$C_{69}H_{64}ClEu_2N_4O_{20.5}$	$C_{69}H_{64}ClEu_2N_4O_{20.5}$	$C_{69}H_{64}ClN_4O_{20.5}Tb_2$	$C_{69}H_{64}ClN_4O_{20.5}Tb_2$
FW	1616.61	1616.61	1630.53	1630.53
T/K	120	120	120	120
Cry. system	monoclinic	monoclinic	monoclinic	monoclinic
Space group	$P2_1$	$P2_1$	$P2_1$	$P2_1$
a /Å	13.7229(8)	13.6925(2)	13.7334(5)	13.6917(7)
b /Å	28.1271(19)	28.1386(4)	28.0916(7)	28.1150(14)
c /Å	17.3870(10)	17.4098(2)	17.3794(6)	17.3468(9)
α/°	90	90	90	90
β/°	99.673(5)	99.5968(13)	99.823(3)	99.903(4)
γ/°	90	90	90	90
V/Å^3	6615.7(7)	6613.88(16)	6606.6(4)	6578.0(6)
Z	4	4	4	4
ρ_c/g cm^{-3}	1.623	1.624	1.639	1.646
μ/ mm^{-1}	14.475	14.479	11.432	11.481
Data/parameters	17660/1746	21356/1747	19131/1747	21994/1741
2θ/°	6.038-129.994	5.148-129.982	7.252-139.242	6.052-133
Obs. reflections	38793	65693	74197	61886
F(000)	3252.0	3252.0	3268.0	3268.0
GOF	1.073	1.028	1.014	1.125
R_1[I> 2σ(I)][a]	0.0528	0.0727	0.0815	0.0880
wR_2(All data)[b]	0.1278	0.0897	0.2268	0.2318

[a]$R_1=\Sigma||F_O| - |F_C||/\Sigma|F_O|$; [b]$wR_2=\{\Sigma[w(F_O^2 - F_C^2)^2]/\Sigma[w(F_O^2)^2]\}^{1/2}$

Table S3. Selected bond distances (Å) and band angles (°) of ***R*-Eu**.

Eu1-O1[1]	2.490(9)	Eu1-O5	2.411(9)
Eu1-O2	2.322(9)	Eu1-O6	2.467(10)
Eu1-O3[2]	2.515(8)	Eu1-O8[2]	2.372(9)
Eu1-O4	2.319(10)	Eu1-O9[1]	2.352(8)
Symmetry code:[1]-1/2+X,3/2-Y,1-Z; [2]1+X,+Y,+Z.			
O1[1]-Eu1-O3[2]	138.1(3)	C10-O1-Eu1[3]	120.7(5)
O2-Eu1-O1[1]	125.4(3)	C11-O1-Eu1[3]	126.0(7)
O2-Eu1-O3[2]	81.9(3)	C6-O2-Eu1	153.2(7)
O2-Eu1-O5	74.5(4)	C8-O3-Eu1[4]	119.3(5)
O2-Eu1-O6	74.1(3)	C9-O3-Eu1[4]	123.7(8)
O2-Eu1-O8[2]	137.0(3)	C16-O4-Eu1	155.3(8)
O2-Eu1-O9[1]	82.3(3)	C6-O8-Eu1[4]	123.0(7)
O4-Eu1-O1[1]	78.4(3)	C16-O9-Eu1[3]	125.4(6)
O4-Eu1-O2	139.3(4)	O5-Eu1-O6	145.0(3)
O4-Eu1-O3[2]	101.4(3)	O6-Eu1-O1[1]	137.5(3)
O4-Eu1-O5	145.9(3)	O6-Eu1-O3[2]	75.6(3)
O4-Eu1-O6	67.8(3)	O8[2]-Eu1-O1[1]	77.3(3)
O4-Eu1-O8[2]	75.1(3)	O8[2]-Eu1-O3[2]	62.7(3)
O4-Eu1-O9[1]	80.7(4)	O8[2]-Eu1-O5	78.6(3)
O5-Eu1-O1[1]	75.0(3)	O8[2]-Eu1-O6	115.8(3)
O5-Eu1-O3[2]	84.9(3)	O9[1]-Eu1-O1[1]	64.3(3)
O9[1]-Eu1-O6	84.8(3)	O9[1]-Eu1-O3[2]	157.6(3)
O9[1]-Eu1-O8[2]	137.9(3)	O9[1]-Eu1-O5	105.9(3)

Symmetry code:[1]-1/2+X,3/2-Y,1-Z; [2]1+X,+Y,+Z; [3]1/2+X,3/2-Y,1-Z; [4]-1+X,+Y,+Z.

Table S4. Selected bond distances (Å) and band angles (°) of ***S*-Eu**.

Eu1-O8[1]	2.502(4)	Eu1-O1	2.409(4)
Eu1-O4	2.320(4)	Eu1-O6[1]	2.342(4)
Eu1-O2	2.327(3)	Eu1-O3	2.476(4)
Eu1-O7[2]	2.511(4)	Eu1-O5[2]	2.365(4)
Symmetry code:[1]3/2-X,1-Y,1/2+Z; [2]+X,+Y,-1+Z.			
O8[1]-Eu1-O7[2]	137.97(12)	O5[2]-Eu1-O1	78.47(14)
O4-Eu1-O8[1]	78.80(13)	O5[2]-Eu1-O3	115.86(14)
O4-Eu1-O2	139.40(15)	O1-Eu1-O8[1]	75.05(13)
O4-Eu1-O7[2]	100.89(14)	O1-Eu1-O7[2]	84.83(14)
O4-Eu1-O1	146.00(14)	O1-Eu1-O3	144.94(14)
O4-Eu1-O6[1]	81.07(14)	O2-Eu1-O3	74.21(14)
O4-Eu1-O3	67.54(14)	O2-Eu1-O5[2]	137.00(13)
O4-Eu1-O5[2]	74.73(14)	O6[1]-Eu1-O8[1]	64.95(12)
O5[2]-Eu1-O8[1]	76.94(12)	O6[1]-Eu1-O7[2]	157.08(13)
O5[2]-Eu1-O7[2]	62.92(12)	O6[1]-Eu1-O1	106.45(15)
O2-Eu1-O8[1]	125.54(13)	O6[1]-Eu1-O3	84.38(14)
O2-Eu1-O7[2]	81.78(13)	O6[1]-Eu1-O5[2]	138.04(13)
O2-Eu1-O1	74.43(15)	O3-Eu1-O8[1]	137.56(13)
O2-Eu1-O6[1]	82.20(13)	O3-Eu1-O7[2]	75.55(13)
O8[1]-Eu1-O7[2]	137.97(12)	O5[2]-Eu1-O1	78.47(14)
O4-Eu1-O8[1]	78.80(13)	O5[2]-Eu1-O3	115.86(14)
O4-Eu1-O2	139.40(15)	O1-Eu1-O8[1]	75.05(13)
O4-Eu1-O7[2]	100.89(14)	O1-Eu1-O7[2]	84.83(14)

Symmetry code:[1]3/2-X,1-Y,1/2+Z; [2]+X,+Y,-1+Z; [3]3/2-X,1-Y,-1/2+Z; [4]+X,+Y,1+Z.

Table S5. Selected bond distances (Å) and band angles (°) of ***R*-Tb**.

Tb1-O1[1]	2.480(7)	Tb1-O7[2]	2.372(7)
Tb1-O2	2.300(7)	Tb1-O8	2.352(7)
Tb1-O3	2.307(7)	O1-Tb1[3]	2.480(7)
Tb1-O4[1]	2.310(7)	O4-Tb1[3]	2.310(7)
Tb1-O5	2.411(7)	O6-Tb1[4]	2.343(7)
Tb1-O6[2]	2.467(7)	O7-Tb1[4]	2.484(7)
Symmetry code: [1]1/2-X,1-Y,1/2+Z; [2]+X,+Y,-1+Z; [3]1/2-X,1-Y,-1/2+Z; [4]+X,+Y,1+Z.			
O1[1]-Tb1-O7[2]	137.6(32)	O2-Tb1-O1[1]	78.7 (3)
O2-Tb1-O3	139.6(3)	C14-O2-Tb1	155.3(6)
O2-Tb1-O4[1]	80.5(3)	C3-O3-Tb1	152.8(6)
O2-Tb1-O5	145.8(3)	C14-O4-Tb1[3]	125.5(5)
O2-Tb1-O6[2]	74.9(3)	C3-O6-Tb1[4]	124.0(6)
O2-Tb1-O7[2]	101.6(3)	O2-Tb1-O8	67.8(3)
O3-Tb1-O1[1]	125.4(3)	O4[1]-Tb1-O8	84.0(3)
O3-Tb1-O4[1]	82.1(3)	O5-Tb1-O1[1]	75.0(3)
O3-Tb1-O5	74.4(3)	O5-Tb1-O7[2]	84.0(3)
O3-Tb1-O6[2]	137.0(2)	O5-Tb1-O8	144.8(2)
O3-Tb1-O7[2]	81.6(2)	O6[2]-Tb1-O1[1]	76.6(2)
O3-Tb1-O8	74.4(3)	O6[2]-Tb1-O5	78.0(3)
O4[1]-Tb1-O1[1]	65.7(2)	O6[2]-Tb1-O7[2]	63.1(2)
O4[1]-Tb1-O5	107.5(3)	O6[2]-Tb1-O8	115.9(3)
O4[1]-Tb1-O6[2]	138.2(3)	O8-Tb1-O1[1]	138.0(2)
O4[1]-Tb1-O7[2]	156.7(3)	O8-Tb1-O7[2]	75.6(3)

Symmetry code: [1]1/2-X,1-Y,1/2+Z; [2]+X,+Y,-1+Z; [3]1/2-X,1-Y,-1/2+Z; [4]+X,+Y,1+Z.

Table S6. Selected bond distances (Å) and band angles (°) of ***S*-Tb**.

Tb1-O1[1]	2.476(6)	Tb1-O5	2.411(6)
Tb1-O2[2]	2.479(6)	Tb1-O6	2.292(6)
Tb1-O3	2.369(6)	Tb1-O7	2.432(7)
Tb1-O4[1]	2.305(6)	Tb1-O8[2]	2.343(6)
Symmetry code: [1]1/2-X,1-Y,1/2+Z; [2]+X,+Y,-1+Z.			
O1[1]-Tb1-O2[2]	138.3(2)	O3-Tb1-O1[1]	74.6 (2)
O3-Tb1-O2[2]	85.0(2)	O3-Tb1-O7	145.0(2)
O4[1]-Tb1-O1[1]	65.4(2)	C12-O4-Tb1[3]	124.9(5)
O4[1]-Tb1-O2[2]	156.2(2)	C6-O5-Tb1	152.2(6)
O4[1]-Tb1-O3	106.4(2)	C12-O6-Tb1	154.2(6)
O4[1]-Tb1-O7	83.9(2)	C6-O8-Tb1[4]	124.4(6)
O8[2]-Tb1-O2[2]	63.6(2)	O8[2]-Tb1-O7	116.3(2)
O8[2]-Tb1-O1[1]	76.7(2)	O8[2]-Tb1-O3	78.3(2)
O4[1]-Tb1-O8[2]	138.3(2)	O7-Tb1-O2[2]	75.4(2)
O5-Tb1-O1[1]	82.1(3)	O7-Tb1-O1[1]	137.8(2)
O5-Tb1-O2[2]	81.4(2)	O6-Tb1-O8[2]	74.9 (2)
O5-Tb1-O3	74.4(2)	O6-Tb1-O7	67.4(2)
O5-Tb1-O4[1]	81.8(2)	O6-Tb1-O2[2]	101.0(2)
O5-Tb1-O7	74.2(2)	O6-Tb1-O3	146.1(2)
O5-Tb1-O8[2]	137.0(2)	O6-Tb1-O4[1]	81.2(2)
O6-Tb1-O1[1]	79.3(2)	O6-Tb1-O5	139.3(2)
O4[1]-Tb1-O6[2]	138.2(3)	O8-Tb1-O1[1]	138.0(2)
O4[1]-Tb1-O7[2]	156.7(3)	O8-Tb1-O7[2]	75.6(3)

Symmetry code: [1]1/2-X,1-Y,1/2+Z; [2]+X,+Y,-1+Z; [3]1/2-X,1-Y,-1/2+Z; [4]+X,+Y,1+Z.

Table S7. Selected bond distances (Å) and band angles (°) of ***R*-Eu-phen**.

Eu1-O3	2.403(9)	Eu1-O16	2.349(10)
Eu1-O9	2.402(8)	Eu1-O20	2.601(9)
Eu1-O12	2.293(9)	Eu1-O21	2.938(9)
Eu1-O15	2.359(9)	Eu1-N3	2.604(11)
Symmetry code: [1]+X,+Y,-1+Z; [2]+X,+Y,1+Z.			
O3-Eu1-O20	69.9(3)	O12-Eu1-O15	78.8(3)
O3-Eu1-O21	47.5(3)	O12-Eu1-O16	77.5(3)
O3-Eu1-N3	141.4(4)	O12-Eu1-O20	150.0(3)
O3-Eu1-N8	138.6(3)	O12-Eu1-O21	77.0(3)
O9-Eu1-O3	74.7(3)	O12-Eu1-N3	84.2(3)
O9-Eu1-O20	62.2(3)	O12-Eu1-N8	81.1(3)
O9-Eu1-O21	116.4(3)	N8-Eu1-O21	142.7(3)
O9-Eu1-N3	98.6(3)	N8-Eu1-O20	105.3(3)
O9-Eu1-N8	67.7(3)	O12-Eu1-O9	142.8(3)
O12-Eu1-O3	124.3(3)	N3-Eu1-O21	141.9(3)
O20-Eu1-N3	73.4(3)	O16-Eu1-O3	77.7(3)
O20-Eu1-O21	108.8(3)	O15-Eu1-N8	138.7(3)
O16-Eu1-N8	77.4(3)	O15-Eu1-N3	79.0(3)
O16-Eu1-N3	138.7(3)	O15-Eu1-O21	65.0(3)
O16-Eu1-O21	68.7(3)	O15-Eu1-O20	77.6 (3)
O16-Eu-O20	132.4(3)	O15-Eu1-O9	138.3(3)
O16-Eu1-O15	131.4(3)	O16-Eu1-O9	76.3(3)

Symmetry code: [1]+X,+Y,-1+Z; [2]+X,+Y,1+Z.

Table S8. Selected bond distances (Å) and band angles (°) of ***S*-Eu-phen**.

Eu1-N2	2.597(16)	Eu1-O10	2.372(11)
Eu1-O1	2.393(13)	Eu1-O19	2.371(12)
Eu1-N3	2.588(15)	Eu1-O25	2.408(11)
Eu1-O2	2.961(13)	Eu1-O26	2.599(10)
Symmetry code: [1]+X,+Y,1+Z; [2]+X,+Y,-1+Z.			
O1-Eu1-O2	142.7(4)	N2-Eu1-O26	106.0(4)
O1-Eu1-N2	139.0(4)	O1-Eu1-N3	141.0(4)
O1-Eu1-O2	47.2(4)	O1-Eu1-O25	75.0(4)
O1-Eu1-O26	69.3(4)	N3-Eu1-N2	63.5(5)
N3-Eu1-O2	141.9(4)	N3-Eu1-O26	73.7(4)
O10-Eu1-N2	139.1(4)	O10-Eu1-O1	81.1(4)
O10-Eu1-N3	79.2(4)	O10-Eu1-O2	64.8(4)
O10-Eu1-O25	137.8(4)	O10-Eu1-O26	77.1(3)
O19-Eu1-N2	77.2(5)	O19-Eu1-O1	77.9(4)
O19-Eu1-N3	138.9(4)	O19-Eu1-O2	68.8(4)
O19-Eu1-O10	131.6(4)	O19-Eu1-O25	76.4(4)
O19-Eu1-O26	132.0(4)	O25-Eu1-N2	67.9(4)
O25-Eu1-N3	98.3(4)	O25-Eu1-O2	116.4(4)
O25-Eu1-O26	62.1(3)	O26-Eu1-O2	108.0(4)
O36-Eu1-N2	81.1(5)	O36-Eu1-O1	123.9(4)
O36-Eu1-N3	84.6(5)	O36-Eu1-O2	77.0(4)
O36-Eu1-O10	79.1(4)	O36-Eu1-O19	77.5(4)
Symmetry code: [1]+X,+Y,-1+Z; [2]+X,+Y,1+Z.			

Table S9. Selected bond distances (Å) and band angles (°) of ***R*-Tb-phen**.

Tb1-O1	2.308(12)	Tb1-O4	2.415(13)
Tb1-O2[1]	2.427(13)	Tb1-O13	2.358(14)
Tb1-O14	2.361(13)	Tb1-N1	2.575(18)
Tb1-O31	2.364(14)	Tb1-N5	2.565(17)
Symmetry code: [1]+X,+Y,1+Z; [2]+X,+Y,-1+Z.			
O1-Tb1-O2[1]	88.5(4)	O1-Tb1-O4	84.5(5)
O1-Tb1-O13	73.4(5)	O1-Tb1-O14	72.5(5)
O1-Tb1-N1	146.7(5)	O1-Tb1-O31	113.3(5)
O1-Tb1-N5	149.0(5)	O2[1]-Tb1-N1	69.0(5)
O2[1]-Tb1-N5	107.0(5)	O4-Tb1-O2[1]	72.9(4)
O4-Tb1-N1	110.2(5)	O4-Tb1-N5	75.1(5)
O13-Tb1-O2[1]	144.2(5)	O13-Tb1-O4	74.8(5)
O13-Tb1-O14	125.5(5)	O13-Tb1-N1	138.3(5)
O13-Tb1-O31	78.8(5)	O13-Tb1-N5	78.7(5)
O14-Tb1-O2[1]	74.8(4)	O14-Tb1-O4	140.4(5)
O14-Tb1-N1	77.9(5)	O14-Tb1-O31	77.4(5)
O14-Tb1-N5	136.9(5)	O31-Tb1-O2[1]	137.0(5)
O31-Tb1-O4	142.1(5)	O31-Tb1-N1	73.6(5)
O31-Tb1-N5	73.4(5)	N5-Tb1-N1	63.9(6)
O5-Tb2-O7	124.3(5)	O5-Tb2-O10	77.8(5)
O5-Tb2-O12	78.9(5)	O5-Tb2-O16	142.1(5)
O5-Tb2-O21	150.0(5)	O5-Tb2-N4	82.9(5)
O5-Tb2-N8	79.1(5)	O7-Tb2-O16	75.6(5)

Symmetry code: [1]+X,+Y,1+Z; [2]+X,+Y,-1+Z.

Table S10. Selected bond distances (Å) and band angles (°) of ***S*-Tb-phen**.

Tb1-O6[1]	2.425(17)	Tb1-O13	2.385(18)
Tb1-O15	2.417(17)	Tb1-O16	2.391(16)
Tb1-O19	2.340(17)	Tb1-O27	2.321(17)
Tb1-N3	2.59(2)	Tb1-N5	2.56(2)
Symmetry code: [1]+X,+Y,-1+Z; [2]+X,+Y,1+Z.			
O6[1]-Tb1-N3	105.1(6)	O6[1]-Tb1-N5	65.0(6)
O13-Tb1-O6[1]	73.7(6)	O13-Tb1-O15	75.5(6)
O13-Tb1-O16	74.9(6)	O13-Tb1-N3	71.5(6)
O13-Tb1-N5	105.7(6)	O15-Tb1-O6[1]	76.9(6)
O15-Tb1-N5	139.1(7)	O16-Tb1-O6[1]	145.1(5)
O15-Tb1-N3	144.6(7)	O16-Tb1-O15	81.0(6)
O16-Tb1-N3	78.5(6)	O16-Tb1-N5	139.6(6)
O19-Tb1-O6[1]	76.4(6)	O19-Tb1-O13	145.8(6)
O19-Tb1-O15	82.0(6)	O19-Tb1-O16	126.8(6)
O19-Tb1-N3	133.2(6)	O19-Tb1-N5	75.4(6)
O27-Tb1-O6[1]	141.9(6)	O27-Tb1-O13	139.9(6)
O27-Tb1-O15	121.4(6)	O27-Tb1-O16	72.9(6)
O27-Tb1-O19	74.0(6)	O27-Tb1-N3	79.2(6)
O27-Tb1-N5	84.6(6)	N5-Tb1-N3	64.3(7)
O1-Tb2-N6	67.7(6)	O1-Tb2-N8	106.3(6)
O2-Tb2-O1	90.3(5)	O2-Tb2-O3	72.2(6)
O2-Tb2-O12	85.2(6)	O2-Tb2-O32	73.1(6)

Symmetry code: [1]+X,+Y,-1+Z; [2]+X,+Y,1+Z.

Table S11 The calculated value of CShM for Ln^{3+} of ***R*/*S*-Ln** (Ln = Eu/Tb).

Structure	***R*-Eu**	***S*-Eu**	***R*-Tb**	***S*-Tb**
	Eu1	**Eu1**	**Tb1**	**Tb1**
OP-8	30.466	30.352	30.67	30.44
HPY-8	26.7	26.755	26.896	26.933
HBPY-8	28.922	28.963	29.169	29.237
CU-8	28.735	28.770	28.931	29.049
SAPR-8	24.461	24.384	24.711	24.595
TDD-8	22.629	22.554	22.773	22.755
JGBF-8	24.688	24.727	24.883	24.793
JETBPY-8	**13.252**	**13.219**	**13.314**	**13.344**
JBTPR-8	17.33	17.218	17.439	17.367
BTPR-8	21.976	21.852	22.13	22.052
JSD-8	17.46	17.398	17.647	17.501
TT-8	29.214	29.272	29.452	29.553
ETBPY-8	22.601	22.525	22.77	22.777

Table S12 The calculated value of CShM for Ln^{3+} of ***R*/*S*-Ln-phen** (Ln = Eu/Tb).

Structure	***R*-Eu-phen**				***S*-Eu-phen**			
	Eu1	**Eu2**	**Eu3**	**Eu4**	**Eu1**	**Eu2**	**Eu3**	**Eu4**
EP-9	25.841	27.827	24.608	25.045	25.975	25.118	28.001	24.373
OPY-9	16.273	17.538	15.127	17.683	16.327	17.559	17.414	15.229
HBPY-9	20.4	19.238	20.319	22.958	20.588	22.644	18.94	20.321
JTC-9	21.847	21.874	16.965	17.275	21.962	17.086	21.721	16.651
JCCU-9	14.966	15.225	16.123	16.794	14.96	17.085	15.319	16.2922
CCU-9	17.879	18.092	15.776	17.171	17.924	17.316	18.158	16.011
JCSAPR-9	**10.883**	**10.855**	10.138	9.031	**10.944**	9.158	**10.762**	10.432
CSAPR-9	13.089	13.038	9.747	9.351	13.2	9.344	12.924	9.953
JTCTPR-9	12.297	12.472	11.535	9.558	12.288	9.757	12.364	11.808
TCTPR-9	14.379	14.466	10.554	10.41	14.475	10.415	14.403	10.801
JTDIC-9	20.166	20.487	18.067	18.27	20.143	18.432	20.524	18.034
HH-9	18.03	17.101	14.417	15.634	18.207	15.671	16.915	14.521
MFF-9	12.217	11.95	**8.807**	**8.537**	12.31	**8.539**	11.81	**9.024**

Structure	***R*-Tb-phen**				***S*-Tb-phen**			
	Tb1	**Tb2**	**Tb3**	**Tb4**	**Tb1**	**Tb2**	**Tb3**	**Tb4**
EP-9	25.365	26.049	24.603	27.73	27.636	25.096	26.02	24.775
OPY-9	17.869	16.731	15.036	17.932	18.464	18.096	16.767	15.143
HBPY-9	22.907	20.879	19.671	19.672	19.959	23.188	20.88	20.091
JTC-9	17.538	22.269	16.811	22.085	22.065	17.27	22.405	17.025
JCCU-9	16.233	15.068	15.94	15.637	15.452	16.136	15.238	15.851
CCU-9	17.095	18.217	15.703	18.779	18.62	16.901	18.353	15.601
JCSAPR-9	8.536	**11.149**	9.584	**11.273**	**11.325**	8.692	**11.281**	9.752
CSAPR-9	9.292	13.592	9.273	13.718	13.787	9.368	13.699	9.407

JTCTPR-9	9.137	12.564	11.131	12.846	12.809	9.218	12.736	11.266
TCTPR-9	10.371	14.875	9.928	15.2208	15.378	10.489	14.969	10.102
JTDIC-9	18.341	20.065	18.326	20.763	20.888	18.198	20.127	18.25
HH-9	15.747	18.394	14.311	17.785	17.959	15.544	18.402	14.331
MFF-9	**8.534**	12.74	**8.378**	12.617	12.642	**8.56**	14.331	**8.473**

Table S13 The g_{lum} values of ***R*/*S*-Eu** and ***R*/*S*-Eu-phen**.

Structure	$^5D_0 \rightarrow {}^7F_1$	$^5D_0 \rightarrow {}^7F_2$	$^5D_0 \rightarrow {}^7F_3$	$^5D_0 \rightarrow {}^7F_4$
***R*-Eu**	$-7.3*10^{-4}$	0.0011	0.0061	-0.0039
***S*-Eu**	$7.3*10^{-4}$	-0.0010	-0.0060	0.0053
***R*-Eu-phen**	-0.0036	-0.0017	0.0010	$7.4*10^{-4}$
***S*-Eu-phen**	0.0040	0.0018	-0.0056	-0.0012

Table S14 The g_{lum} values of ***R*/*S*-Tb** and ***R*/*S*-Tb-phen**.

Structure	$^5D_4 \rightarrow {}^7F_6$	$^5D_4 \rightarrow {}^7F_5$	$^5D_4 \rightarrow {}^7F_4$	$^5D_4 \rightarrow {}^7F_3$
***R*-Tb**	0.0012	$-9.7*10^{-4}$	0.0031	-0.0011
***S*-Tb**	-0.0017	$9.7*10^{-4}$	-0.0013	-0.0011
***R*-Tb-phen**	$-4.1*10^{-4}$	0.0012	$3.1*10^{-4}$	$-2.3*10^{-4}$
***S*-Tb-phen**	$2.2*10^{-4}$	-0.0012	$-4.8*10^{-4}$	$2.3*10^{-4}$

References

1 L. J. Bourhis, O. V. Dolomanov, R. J. Gildea, J. A. K. Howard, and H. Puschmann, The anatomy of a comprehensive constrained, restrained refinement program for the modern computing environment - Olex2 dissected, *Acta Crystallogr., Sect. A: Cryst. Phys., Diffr., Theor. Gen. Crystallogr.*, 2015, **71**, 59.

2 H. Zhao and P. Schuck, Combining biophysical methods for the analysis of protein complex stoichiometry and affinity in SEDPHAT, *Acta Crystallogr., Sect. D: Biol. Crystallogr.*, 2015, **71**, 3.

3 P. Raithby, Acta Crystallographica Section C: Chemistry Matters, *Acta Crystallogr., Sect. C: Cryst. Struct. Commun.*, 2023, **79**, 25.